NASA TECHNICAL MEMORANDUM 102699

CHARACTERIZATION OF UNNOTCHED SCS-6/Ti-15-3 METAL MATRIX COMPOSITES AT 650°C

W. D. Pollock and W. Steven Johnson

SEPTEMBER 1990

National Aeronautics and
Space Administration

Langley Research Center
Hampton, Virginia 23665-5225

CHARACTERIZATION OF UNNOTCHED SCS-6/Ti-15-3 METAL MATRIX COMPOSITES AT 650°C

W. D. Pollock* and W. S. Johnson**
NASA Langley Research Center
Hampton, Virginia

INTRODUCTION

New aerospace vehicles are pushing the capabilities of current materials to their limit. Proposed supersonic and hypersonic vehicles require light weight materials with good mechanical properties at elevated temperatures. Titanium has better mechanical properties at elevated temperature than aluminum, and although not as light, it is much lighter than most other candidate materials. To improve the strength and stiffness at elevated temperatures and keep the weight low, reinforcement has been added to the titanium. The most common reinforcement is the silicon carbide (SiC) fiber. The system used in this research was the Ti-15-3 (15 weight% vanadium, 3 weight% aluminum, 3 weight% chromium, and 3 weight% tin [1]) matrix reinforced with continuous SCS-6 SiC fibers.

The objectives of this research were to gain an understanding of the response of the composite to applied loads at elevated temperature, to compare this behavior to previously obtained room temperature results [2] and to evaluate an analytical technique for predicting composite behavior at elevated temperature using constituent properties. The current research evaluated the response of the composite to monotonic and cyclic loading at elevated temperature. Curves of maximum stress against fatigue life were generated for several lay-ups. Analytical methods were used to predict the response of the composite to various loading histories using the constituent properties. Damage initiation and propagation were studied and related to the microstructure and load history.

* Materials Engineer, Analytical Services and Materials, Inc.
** Senior Research Engineer

MATERIALS AND EXPERIMENTAL PROCEDURES

Material

The SiC fibers, designated SCS-6 by the manufacturer (Textron Specialty Materials), are 0.145 mm in diameter with an elastic modulus of 412 GPa and an ultimate tensile strength of 3.5 to 4.4 GPa [3]. The fibers were laid up between the matrix foils and consolidated by hot pressing. Four different 8-ply lay-ups were tested: $[0]_8$, $[0/90]_{2S}$, $[0_2/\pm45]_S$, $[0/\pm45/90]_S$. In addition, a 13-ply panel was made of foils only and processed the same as the composite panels. This material will be referred to as foil matrix material. This provided an unreinforced matrix subjected to the same processing as the composite. Thicker Ti-15-3 matrix material was also acquired from the same vendor as the foil (Timet). The thicker material will be referred to as plate matrix material. The composite specimens and foil matrix specimens tested at elevated temperature were straight sided, 0.20 cm thick, 15.2 cm long and 1.3 cm wide. The plate matrix specimens were 0.5 cm thick, 1.3 cm wide and 15.2 cm long.

Strain-controlled tests were used to simulate the behavior of the matrix material in the composite. In the strain-controlled cyclic tests, once the maximum strain was achieved, the matrix stress dropped rapidly due to time-dependent deformation. At the minimum strain, compressive loads were required to compensate for the time-dependent deformation. These compressive loads caused the thin foil matrix coupons to buckle. Fixtures to prevent buckling could not be used due to the elevated temperature. Therefore, the thicker plates of matrix were needed for the strain-controlled cyclic tests.

Test Procedures

All tests were conducted in a servohydraulic test frame. The grips were water cooled and the samples were heated by a 5kW induction heater. The temperature was monitored by two infrared pyrometers and a microprocessor controlled the induction heater. All cyclic tests were performed at 10 Hz with an R ratio (P_{min}/P_{max}) of 0.1. The load-controlled monotonic tests were loaded at a rate of 0.273 kN/s. This rate was chosen to match the rate used in the room temperature tests [2]. The strain-controlled monotonic test strain rate was 0.0061 $^{mm}/_{mm}$ per minute. This strain rate matched the load-controlled strain rate of the unidirectional composite at 650°C. The strain was monitored by a water-cooled, high temperature extensometer that had two quartz rods which contact the coupon. An infrared camera was used to monitor the thermal gradient across the test section. The infrared image provides a full field view of the sample as opposed to a thermocouple point reference. With this monitoring method, the gradient at 650°C was reduced to 10°C over a 50 mm length. This length spanned the 25 mm gage length. The maximum load and strain used during the cyclic tests are presented in

Table 1. Due to the shortage of material only one test was conducted for each condition. During the cyclic tests the loading rate of some individual cycles was slowed to 0.5 Hz so the stress-strain curve could be plotted on an x-y recorder. Typically, the stress-strain curve for cycles 1-5,10,20,50,100,500,1000 and so on were recorded.

Test Temperature and Hold Time

A test temperature of 650°C was selected for two reasons. First, this temperature appears to be the highest use temperature considered for this composite. Second, preliminary tests indicated that the matrix material exhibited time-dependent deformation at this temperature. These tests will be described in the next section.

Infrared pyrometers provided the temperature feedback to the controller. This feedback depends on the surface emissivity of the titanium. The emissivity will change with time at temperature as oxides form on the surface. A few tests, using a thermocouple as a reference for calibration, showed that at 650°C the oxide formation and, therefore, the emissivity stabilized after thirty minutes. Therefore, a hold time of at least thirty minutes at 650°C was required before testing to insure stable temperature readings.

It has been shown that this metastable beta alloy exhibits a phase change at elevated temperatures which can affect the mechanical properties [4]. Elevated temperatures also cause reactions at the SiC fiber-titanium matrix interface which can change the response of the composite. There was some concern that these metallurgical changes would cause significant scatter in the experimental results. Differential Scanning Calorimetry (DSC) tests were conducted to study the stability of the composite at 650°C. The DSC measures the heat flow into a sample as a function of time and temperature. The sample was heated to 650°C and held at this temperature for 150 minutes. Since heat flow is required for metallurgical reactions such as phase changes or interfacial reactions, this test will indicate how long it takes a sample to stabilize during an isothermal hold.

Analytical Model

One of the objectives of this research was to evaluate an analytical technique for predicting the mechanical behavior of the titanium matrix composites at elevated temperature using constituent properties. The laminate stress-strain curves to failure were predicted using the AGLPLY program [5], the same program that was used to predict the room temperature mechanical properties [2]. This program performs an elastic-plastic analysis of composite laminated plates under inplane mechanical loads. The program uses the vanishing-fiber-diameter (VFD) model [5] to predict laminate behavior. The VFD model is a

homogeneous, orthotropic material model based on constituent properties. The fiber and matrix properties are input for the analysis. The experimentally observed elastic-plastic stress-strain curves for the matrix material were used with no empirical correction factors. AGLPLY does not predict time-dependent deformation. The model assumes perfect fiber/matrix bonding. Thus, if fiber/matrix interfaces fail this program would predict a somewhat stiffer response than would be experimentally observed. The AGLPLY program computes the overall laminate elastic moduli, the average stresses and strains in the fiber and matrix of each ply, and the overall strains of the composite for the entire loading regime. Laminate properties predicted by the AGLPLY program compared favorably with laminate properties predicted by other material models developed for metal matrix composites [6].

RESULTS AND DISCUSSION

This section will describe the microstructural analysis and compare experimental and predicted results. First, the data used to design the experiments and a study of the microstructure of the composite will be presented. Then the mechanical properties of the matrix, and both experimental and predicted mechanical properties of the composite will be discussed. Lastly, a fractographic study of the matrix and composite after monotonic and cyclic loading will be discussed.

Preliminary tests were performed on the matrix to determine the minimum temperature at which time-dependent deformation is significant. A constant stress of 70 MPa was applied and the temperature was increased incrementally while monitoring the strain. At each temperature level, the temperature was held for one hour. Figure 1 shows the extent of strain for each increment. Although some time-dependent deformation was observed at 480^{o}C, it was not significant. At 650^{o}C, however, there was a significant amount of time-dependent deformation; in fact, the matrix material continued to deform after the hold period of one hour at 650^{o}C. Therefore, by testing at 650^{o}C, time-dependent deformation will occur in the matrix and, thus, must be properly accounted for in the analytical predictions.

DSC analysis was done to study the thermal stability of the composite at 650^{o}C. A DSC scan of the composite is shown in Figure 2. The heat flow, measured by the DSC, increased rapidly during the first 50 minutes of the 650^{o}C isothermal hold and then approached a constant value (i.e., the heat flow rate approached zero). Therefore, in all tests, an initial 50-minute hold time was used. This will result in less scatter in the data due to the relatively low rate at which metallurgical reactions are occurring. This initial hold was also more than sufficient to build an oxide layer for stable emissivity readings.

Composite Microstructure

The microstructure of the as-received $[0]_8$ composite is shown in Figure 3(a). The carbon core of the fibers is visible as well as the carbon-rich coating on the fibers. Many of the in the matrix material grains extend from fiber row to fiber row. These grains consist mainly of metastable beta phase, a bcc (body-centered cubic) crystal. Brittle titanium carbides can form along the prior foil boundaries due to poor processing [7]. Figure 3(b) shows the microstructure of a sample that was held at 650°C for one hour. Small amounts of the alpha phase, an hcp (hexagonal-close packed) crystal, formed during this hold time at temperature. The alpha forms along the grain and subgrain boundaries. The alpha typically has improved tensile strength over the beta, but significantly reduces elongation to failure [4].

Monotonic Response

This section describes the stress-strain response of the matrix and the composite to monotonic loading at both room and elevated temperature. Results from load- and strain-controlled tests are compared for the matrix. The monotonic response of the composite was predicted using the monotonic response of the matrix.

Matrix Material

At both room temperature and 650°C, significant differences were observed in the stress-strain response of the matrix material when testing in load or strain control.

At room temperature the modulus was independent of the control mode, as shown in Table 2, the ultimate tensile strength from the strain-controlled test was 19% lower than from the load-controlled test. Presumably the difference in strength is due to the difference in strain rate after yield. The strain to failure is presented with these results in Table 2.

Figure 4 shows the stress-strain curve of the matrix at 650°C in load and strain control. As at room temperature, the elastic modulus at 650°C was independent of the control mode and the inelastic response of the matrix depended on the control mode. The stress level in the strain-controlled test reached 145 MPa but did not work-harden, that is, the load dropped and plastic deformation continued at a stress below 145 MPa. At this loading rate, a portion of the deformation was time dependent. Under load control, the material did exhibit work-hardening and failed at an ultimate tensile strength of 335 MPa. The strain to failure in both tests exceeded the range of the extensometer, 0.15 mm/mm. The strain-controlled tensile strength at 650°C was 81% lower than at room temperature, while, for the load-controlled test, the tensile strength dropped only 64%. The differences in behavior for load and strain control illustrate the dependence of the matrix on the loading history.

Composite

This section describes the monotonic response of the composite at room and elevated temperature. The room temperature [2] and 650°C data, the initial elastic modulus, strain to failure, and ultimate tensile strength, for each lay-up are given in Table 2.

For all lay-ups tested, the initial elastic modulus at elevated temperature was 15 to 22% lower than the initial elastic modulus at room temperature. The amount of drop in initial elastic modulus due to elevated temperature was primarily a function of the percentage of fibers in the loading or 0° direction. However, the angle of the remaining plies also affected how much the initial elastic modulus decreased due to elevated temperature. The 90° fibers have essentially no length along the loading axis and, therefore, contribute little to the modulus of the composite. The 45° fibers are not in the loading direction, but do contribute to the elastic modulus of the composite. The load transferred to the 45° fibers is a function of the yield strength and modulus of the matrix material. The modulus of lay-ups with 45° fibers was more sensitive to a temperature increase because of the reduction in the matrix yield strength and modulus. For instance, both the $[0_2/\pm45]_s$ and the $[0/90]_{2s}$ have the same percentage of fibers in the loading direction, but the $[0_2/\pm45]_s$ had the larger drop in initial elastic modulus due to elevated temperature.

As was the case for the modulus, the strengths at elevated temperature were lower than the strengths at room temperature for all lay-ups. The decrease in strength is primarily a function of the percentage of fibers in the loading direction.

In general, the data in Table 2 show that at room temperature only the unidirectional laminate has a tensile strength that is significantly greater than the matrix material alone. However, at 650°C the yield strength of the matrix material was so low that all of the laminate strengths were significantly greater than the matrix alone. This is one reason that fiber reinforcement is needed for high temperature applications.

Bhatt [9] showed little degradation of the elastic modulus or ultimate tensile strength of the SCS-6 fiber up to 1100°C. The strains to failure of all the composites at elevated temperature were less than at room temperature, as shown in Table 2. The strain to failure can be multiplied by the fiber modulus to estimate the static strength of the 0° fibers. Therefore, assuming the fiber modulus was constant with temperature, the in-situ strength of the fibers was reduced due to exposure to elevated temperature. The strengths reported by Bhatt [9] were from tests done on single fibers (i.e., the fiber not in contact with matrix). Apparently reactions between the fiber and matrix at elevated temperature lowered the strength of the in-situ fiber.

At room temperature, interfacial failure was seen as a knee in the elastic stress-strain curve [2] occurring well below the yield strength of the matrix material. However, this knee was not observed at elevated temperature. At 650° C the matrix yielded before loading the interface to failure. Thus, when the interface failed, the knee was obscured due to the plastic deformation in the matrix material. Previous work [2,8] indicated that, with thermal aging, the interface strength may increase over that of the as-fabricated composite. Therefore, the interface strength may have been greater as a result of the 650°C conditioning of the specimen for one hour prior to testing.

Analytical Predictions

The experimental and predicted stress-strain behavior of each lay-up at 650°C is presented in Figures 5 thru 8. The predictions were made using the AGLPLY computer program based on the strain-controlled matrix response. Since the predictions made with the strain-controlled matrix material response were in better agreement with the experimental results, only the predictions made from the strain-controlled matrix material response are shown.

The tensile strength of each lay-up at elevated temperature was also predicted using AGLPLY. The failure criterion was defined from the results of the unidirectional test as follows. The AGLPLY program calculated the fiber stress in the $[0]_8$ to be 2630 MPa at an applied load of 948 MPa, the observed failure load of the unidirectional composite at 650°C. Failure was defined as the applied stress required to load the 0° fibers to a stress of 2630 MPa. By definition, the predicted failure stress of the unidirectional composite was 948 MPa. The stress in the 0° fiber was used as a failure criteria rather than the strain to failure so that the resulting laminate strength predictions would be conservative (approximating the correct strength but lower strains to failure). Alternatively, using correct failure strain would have predicted strengths that would have been high. The predicted and experimental failure stresses are also shown in Figures 5 through 8.

Composite Cyclic Response

Figure 9 shows the cycles to failure as a function of maximum stress for the various lay-ups at 650°C. The data for the $[0_2/\pm45]_S$ is not shown; there were a large number of defects in this panel which resulted in large discrepancies in the data. For a given stress level, the unidirectional composite had the longest life, the $[0/90]_{2S}$ was second, and the $[0/\pm45/90]_S$ composite had the shortest life. Clearly, the higher the percentage of fibers in the loading direction, the more fatigue resistant is the composite.

Figure 10 compares the maximum strain versus cycles to failure of the unidirectional composite to the maximum strain versus cycles to failure of the matrix loaded in strain control. The fatigue test of the unidirectional specimen was essentially an in-situ fatigue test of the fibers. For high maximum strains, short lives, the initial damage developed in the fibers and the composite had lower life expectation than the matrix. For low maximum strains, long lives, the initial damage developed in the matrix, and the matrix had lower life expectation than the composite. Where the two curves intersect, both the matrix and the fibers were equally likely to develop fatigue damage. Figure 11 shows typical initial fatigue damage that developed in the unidirectional specimen for short, medium and long lives. As shown in Figure 10, for the unidirectional composite it is possible to partition the damage into fiber- or matrix-dominated regions using the cyclic life curves of the composite and the matrix. During the cyclic tests at 650°C, the strain range decreased during the first ten or so cycles. This was opposite to what was reported for the room temperature tests [2]. The strain range was then constant for the remainder of the life. The constant, or stabilized, strain range was multiplied by the modulus of the fiber to obtain the maximum cyclic stress in the 0° fibers. This fiber stress is plotted against life for each lay-up in Figure 12. Note that the room temperature data [2] fall within a narrow band. While the 650° data were more scattered, they fall in the same general region. Compared to the wide variation in the laminate stress versus life data (see Figure 9 and [2]), the scatter in the 0° fiber stress versus life data was much less. This indicates that the stress in the 0° fibers may be a controlling factor in laminate fatigue life.

Analytical Predictions

The stabilized stress-strain response of a $[0/90]_{2S}$ lay-up at room temperature and elevated temperature under cyclic loading is shown in Figure 13. The curves shown were typical of lay-ups with off-axis plies. The room temperature stress-strain curve was bilinear with the unloading curve coincidental with the loading curve. The stress-strain curve at elevated temperature was nonlinear in both loading and unloading. As explained earlier, this stress-strain curve was recorded at a much slower loading rate than the majority of the fatigue cycles. Once the applied load was reduced to the minimum value, there was a net strain which was probably due to the slow loading rate. During a few of the tests the load was held at the minimum to allow the net strain to recover. In all cases the net strain recovered within a few minutes. The cyclic loading was then resumed. The cyclic response with the hold time is shown in Figure 13. The most notable feature was that the initial unloading modulus was greater than the initial loading modulus.

To understand this composite response a coupon of plate matrix material was cycled in the same manner. Using the same strain

rate and strain range, a coupon of the plate matrix material was cycled at 650°C in strain control at a rate of 0.5 Hz. After the first few cycles the stress-strain response stabilized. The stabilized response is shown in Figure 14. Because the response has stabilized, there are only two components of strain, a time-dependent component and elastic component. When the load is increasing, both components of strain increase. When the load is decreasing, the elastic component decreases, while the time-dependent component increases. These components sum to an initial unloading modulus that is greater then the initial loading modulus.

The stress-strain response of the $[0/90]_{2S}$ was predicted using the stress-strain response of the matrix material. The stress-strain curve for the matrix material was divided into two parts, a loading and unloading curve, and used as the matrix input for the AGLPLY program. The loading portion of the matrix stress-strain curve was idealized as perfectly elastic-plastic in the AGLPLY program. Two composite stress-strain curves were predicted, a tensile curve using the matrix loading stress-strain response, and a compressive curve using the matrix unloading stress-strain response. The compressive curve was attached to the end of tensile curve to predict the response of the $[0/90]_{2S}$ lay-up to the cyclic loading. This predicted curve is shown with the experimental curve in Figure 15. The predicted strain levels were less than the experimental, but the trends were shown correctly. The AGLPLY program correctly predicted the initial unloading modulus to be larger than the loading modulus, and also predicted a final net strain.

Fractography

This section will present the fractography of the matrix and the composite at elevated temperature and relate it to the mechanical response for the various loading histories. The emphasis will be on damage initiation and propagation.

Matrix Material

Monotonic - Tensile testing of the matrix in both load and strain control at elevated temperature resulted in ductile failure. The elongation in the load-controlled test was localized around the fracture surface. This matrix elongation caused necking, creating a ridge at the failure surface. There were dimples from the ductile failure on the ridge. A metallographic section parallel to the loading axis revealed no secondary cracks behind the fracture surface.

During the strain-controlled monotonic test at 650°C, dimples were formed due to the ductile failure. In the strain-controlled test, the coupon did not neck as in the load-controlled test.

Fatigue - In load control, the cyclic test at 650°C exhibited the same type of ductile failure surface as the monotonic test. There were dimples on the ridge formed during necking from the ductile failure. No secondary cracks behind the fracture surface were apparent in the polished section.

The fracture surface shown in Figure 16, typical of the strain-controlled cyclic tests, exhibited a cracked region due to fatigue. The rest of the surface fractured in a ductile manner, similar to the monotonic test. Polishing perpendicular to the loading axis revealed secondary cracks for each strain range. These cracks (a typical crack is shown in Figure 17) were, in all cases, transgranular. Fatigue crack growth occurred in the strain-controlled test because the strain control limited the amount of time-dependent deformation. In contrast, the coupon in a load-controlled test was free to creep and failed in a ductile manner.

Composite

Monotonic - All the monotonic tests of the composite were conducted in load control at 650°C. Monotonic failure of each lay-up exhibited ductile voiding around the ends of the broken 0° fibers; a typical example for $[0/90]_{2S}$ is shown in Figure 18(a). Necking of the matrix between the fibers caused the matrix to pull away from the fibers, forming ridges. Dimples were visible on these ridges indicating ductile failure of the matrix, as shown in Figure 18(b). The channel left by the 90° fiber shown in Figure 18(a) was seen in all lay-ups with 90° plies. The channel was created when the interface failed and the 90° fiber was pulled away.

Fatigue - Table 1 shows the maximum stress and number of cycles to failure for each lay-up tested. First, the characteristics common to all the lay-ups will be discussed. Then the specific characteristics of each lay-up and cyclic test will be presented.

General Characteristics - Each of the lay-ups exhibited two failure morphologies. There were flat regions with matrix fatigue cracks and little, if any, debonding along the length of the fiber as seen in the $[0]_8$ lay-up in Figure 19. The fibers failed close to the plane of the matrix crack. There were also regions similar to monotonic failures ductile matrix failure, pulled-out fiber lengths and fiber-matrix debonding. Fractions of the failure surface would be covered by each failure morphology depending on the number of cycles to failure.

Unidirectional - The unidirectional composite that was cycled at 650°C at a maximum stress of 759 MPa (183,000 cycles to failure, see Table 1) had a flat fracture surface with little fiber pullout and little matrix ductility. The matrix fatigue crack progressed across most of the cross section. Behind the fracture surface there were several long matrix cracks, but few broken

fibers. The strain range of this composite was below the fatigue limit of the fibers, but not of the matrix. Cracks grew long enough in the matrix to eventually break the fibers. Failure of the fibers was probably due to local stress concentrations caused by the matrix crack and/or local environmental attack of the fiber.

The fatigue test with the maximum stress of 848 MPa (44,000 cycles to failure) had a life where both the fibers and the matrix were cracking. There was fatigue crack growth evident on the fracture surface, and several matrix cracks with broken fibers were found behind the fracture surface.

The unidirectional composite that was cycled at a maximum stress of 759 MPa (20,000 cycles to failure) had many broken fibers behind the fracture surface but few matrix cracks. The fracture surface showed only two small regions with fatigue type failure. The rest of the fracture surface exhibited ductile failure with the matrix pulling away from the fibers as in the monotonic failure.

Lay-ups with Off-Axis Plies - Damage in the lay-ups with off-axis plies initiated with interfacial failure between the matrix and fibers. As in the unidirectional composite, the amount of matrix cracking will depend on the applied load range. Fracture surfaces from low maximum stress, long life tests exhibited matrix fatigue cracking. The greater the life the more extensive the matrix cracking.

Figure 20 shows the extent of fatigue crack propagation for a low maximum stress, high life fatigue test. This test was fatigued at a maximum stress of 337 MPa until it failed at 64,000 cycles. The cracks initiated in the 90^{o} ply, then progressed along the length of the 90^{o} fiber. On the fracture surface shown in Figure 20, matrix fatigue cracks were also present in the 45^{o} plies and even in the 0^{o} ply. The ductile regions have the same features as a monotonic failure.

CONCLUSIONS

Ti-15-3 reinforced with SCS-6 silicon carbide fibers, in five different lay-ups, was tested at $650^{o}C$ to determine fatigue life, tensile strength, elastic modulus, elongation to failure, and damage initiation and progression. The elevated temperature results were compared to those previously obtained at room temperature. The monotonic stress-strain response of the laminate and a typical cyclic stress-strain curve loop were predicted using constituent properties. Strain-controlled tests of the matrix at $650^{o}C$ provided input for the predictions. Based on these tests, the following conclusions were formed:

o At elevated temperature the fibers contributed more to the monotonic tensile strength and the fatigue endurance of the laminate than at room temperature since the matrix is relatively weak at the elevated temperature.

o The stress in the 0^{o} fibers dominated the monotonic response of the composite. The 0^{o} fibers contributed more to the elastic moduli than the other constituents and dominated the tensile strength and elongation to failure.

o The static strength of the in-situ fiber decreased when held for an hour and tested at $650^{o}C$, as indicated by the decrease in laminate strain to failure at temperature. This decrease in fiber strength was not observed in single fiber tests at elevated temperature [9].

o Strain-controlled tests of the matrix material better approximated the in-situ composite response than the load-controlled tests. It is important to model the matrix properly when predicting the response of the composite.

o Initial damage developed in either the fibers or the matrix. This damage was partitioned as a function of the life and applied strain range for a unidirectional lay-up. High strains and short lives resulted in only multiple fiber failure with no signs of matrix fatigue cracking. Low strains and long lives resulted in extensive matrix cracking and no fiber breakage away from the fracture surface.

o The cyclic life of the composite was governed by the cyclic stress in the 0^{o} fibers. For each lay-up tested, the 0^{o} fiber stress plotted against the cycles to failure at room and elevated temperature fell within a single band. More scatter was found in the 0^{o} fiber stress vs high temperature fatigue life data than for the room temperature data.

o It was observed that the initial unloading modulus was greater than the initial loading modulus. This was due to elevated-temperature time-dependent deformation of the matrix. This phenomenon was modeled using the cyclic response of the matrix material in strain-control and the elastic response of the fibers.

o The matrix appeared to be too weak to cause fiber-matrix interface failure prior to matrix yielding when tested at $650^{o}C$. The stiffness loss that may be due to interfacial failures was obscured by the matrix yielding. The fiber-matrix interface strength may also increase after being held at the elevated temperature. Thus, the knee observed in room temperature tests was not apparent at the elevated temperature.

REFERENCES

[1] Rosenberg, H.W., "Ti-15-3: A new Cold-Formable Sheet Titanium Alloy," Journal of Metals, Vol. 35, No. 11, Nov. 1986, pp 30-34.

[2] Johnson, W.S., Lubowinski, S.J., and Highsmith, A.L., "Mechanical Characterization of Unnotched SCS-6/Ti-15-3 Metal Matrix Composites at Room Temperature," Thermal and Mechanical Behavior of Ceramic and Metal Matrix Composites, ASTM STP 1080, Kennedy, Moeller, and Johnson, Ed., Philadelphia, PA, 1990.

[3] Wawner, F.E., "Boron and Silicon Carbide/Carbon Fibers," Fibre Reinforcements for Composite Materials, Bunsell, ED., 1988, Elsevier Science Publishers, pp. 416.

[4] Okada, M., Banerjee, D., Williams, J.C., "Tensile Properties of Ti-15V-3Al-3Cr-3Sn Alloy," Titanium Science and Technology, Proceeding of the Fifth International Conference on Titanium, Sept. 10-14, 1984, Eds: Lutjering, G., Zwicker, U., Bunk, W., Vol. 3, pp 1835-1842.

[5] Bahei-El-Din, Y.A., Dvorak, G.J., "Plasticity Analysis of Laminated Composite Plates," ASME Journal of Applied Mechanics, Vol. 49, 1982, pp 740-746.

[6] Bigelow, C.A., Johnson, W.S., Naik, R.A., "A Comparison of Various Micromechanics Models for Metal Matrix Composites," Mechanics of Composite Materials and Structures", Ed: Reddy, J.N., Teply, J.L., ASME, 1989.

[7] Lerch, B. A., Gabb, T.P., MacKay, R.A., "Heat Treatment Study of the SiC/Ti-15-3 Composite System," NASA TP 2970, Jan. 1990.

[8] Naik, R.A., Johnson, W.S., Pollock, W.D., "Effect of High Temperature Cycle on the Mechanical Properties of Silicon Carbide/Titanium Metal Matrix Composites," Proceedings of the American Society for Composites, Symposium on High Temperature Composites, June 13-15, 1989, pp. 94-103.

[9] Bhatt, R.T., Kraitchman, M.D., "Environmental Effects on the Tensile Strength of Chemically Vapor Deposited Silicon Carbide Fibers," NASA TM-86981, April 1985, pp. 13-16.

Layup	*Max stress (strain)	% of ultimate tensile strength	Cycles to failure	Type of control
Matrix plate	214 MPa	80%	4	Load
	172 MPa	65%	150	Load
	131 MPa	50%	37,000	Load
	92 MPa	35%	200,000	Load
	0.0088		2890	Strain
	0.0077		13,300	Strain
	0.0047		109,000	Strain
$[0]_8$	896	95%	20,000	Load
	848	90%	44,000	Load
	759	80%	183,000	Load
$[0/90]_{2s}$	493	95%	100	Load
	466	85%	7,800	Load
	383	70%	40,000	Load
$[0/\pm45/90]_s$	379	90%	50	Load
	337	80%	64,000	Load

* R = 0.1 for load & strain control

Table 1. 650°C fatigue test results.

Layup	Test temp	Ultimate tensile strength, MPa	Initial elastic modulus, GPa	Strain to failure, mm/mm	Type of control
Matrix	RT	934	92		Load
Matrix	RT	754	88	0.1495	Strain
Matrix	650°C	335	76	>0.150	Load
Matrix	650°C	145	77	>0.150	Strain
$[0]_8$	RT	1517	189	0.009	Load
$[0]_8$	650°C	948	178	0.0077	Load
Predicted	650°C	*948	181	0.0066	Load
$[0/90]_{2s}$	RT	945	138	0.0097	Load
$[0/90]_{2s}$	650°C	548	126	0.0070	Load
Predicted	650°C	561	154	0.0065	Load
$[0_2/\pm 45]_s$	RT	1069	156	0.0105	Load
$[0_2/\pm 45]_s$	650°C	554	125	0.0070	Load
Predicted	650°C	565	146	0.0066	Load
$[0/\pm 45/90]_s$	RT	752	134	0.0098	Load
$[0/\pm 45/90]_s$	650°C	421	131	0.0077	Load
Predicted	650°C	411	129	0.0066	Load

* Prediction fit to data to establish ultimate fiber strength = 2630 MPa

Table 2. Mechanical properties of the matrix and the composite at room temperature and 650°C.

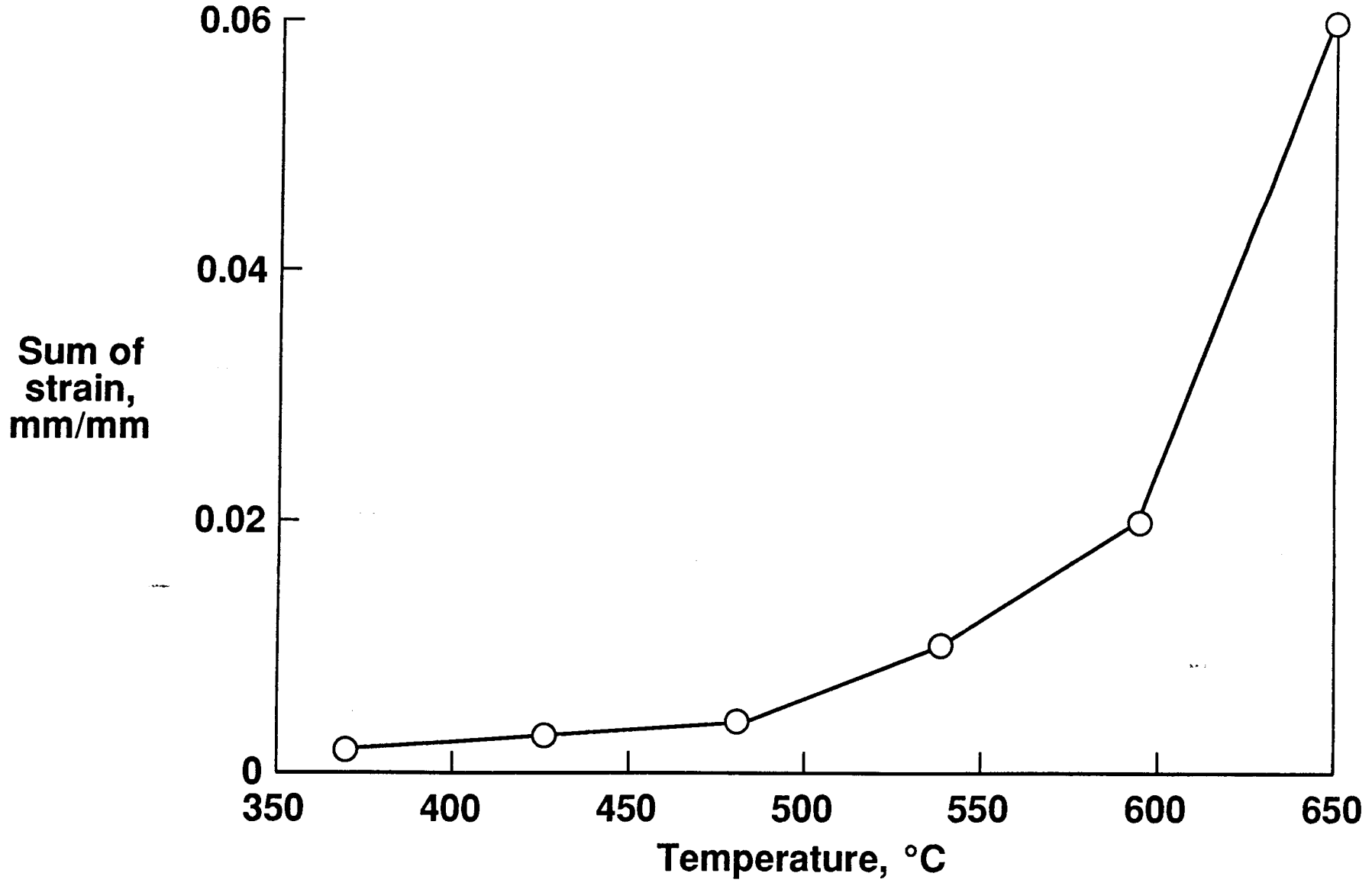

Figure 1. Sum of strain as the temperature is incremented and the load is held constant at 70MPa.

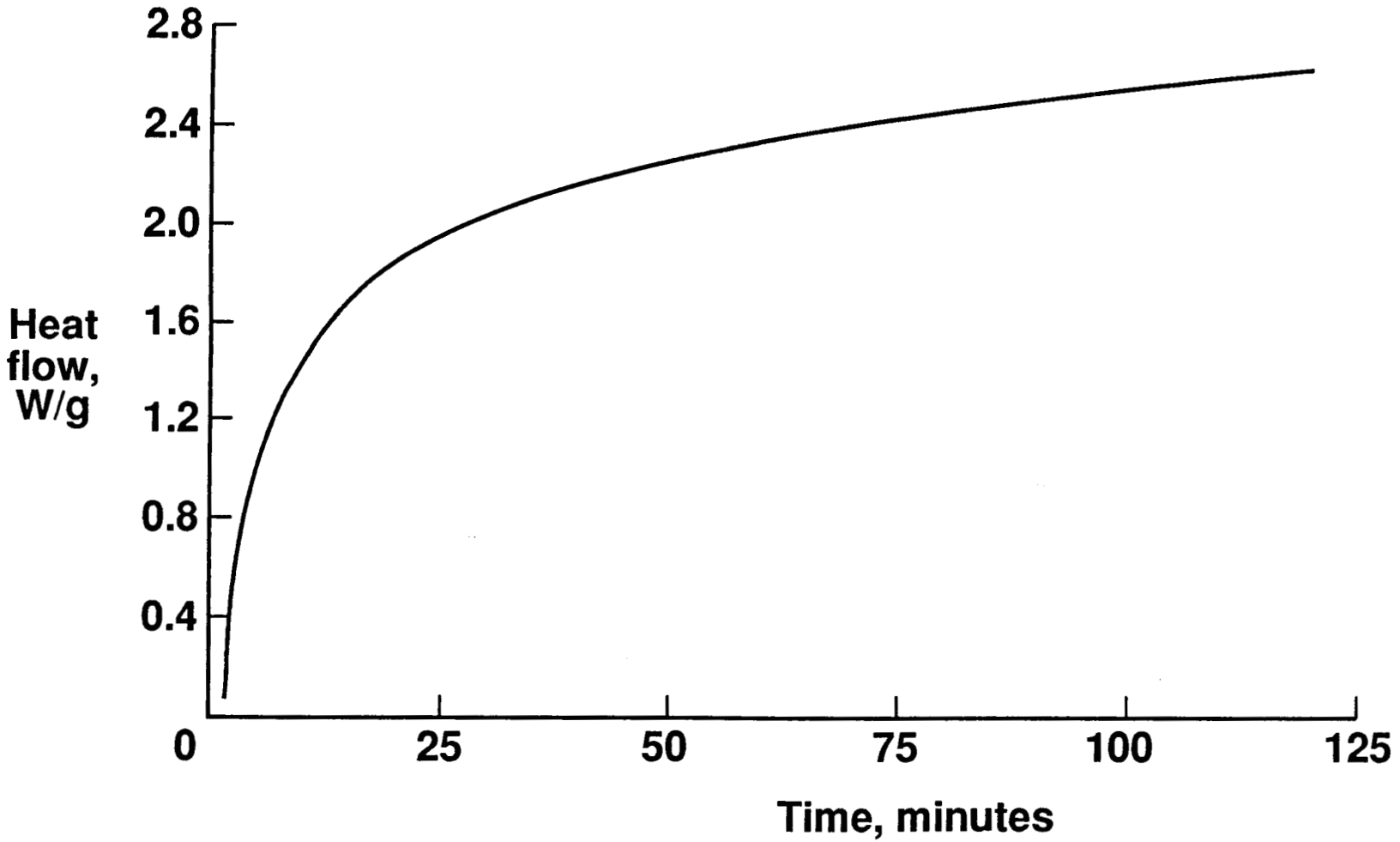

Figure 2. Heat flow into the composite as the temperature was maintained at 650°C, measured by the differential scanning calorimeter.

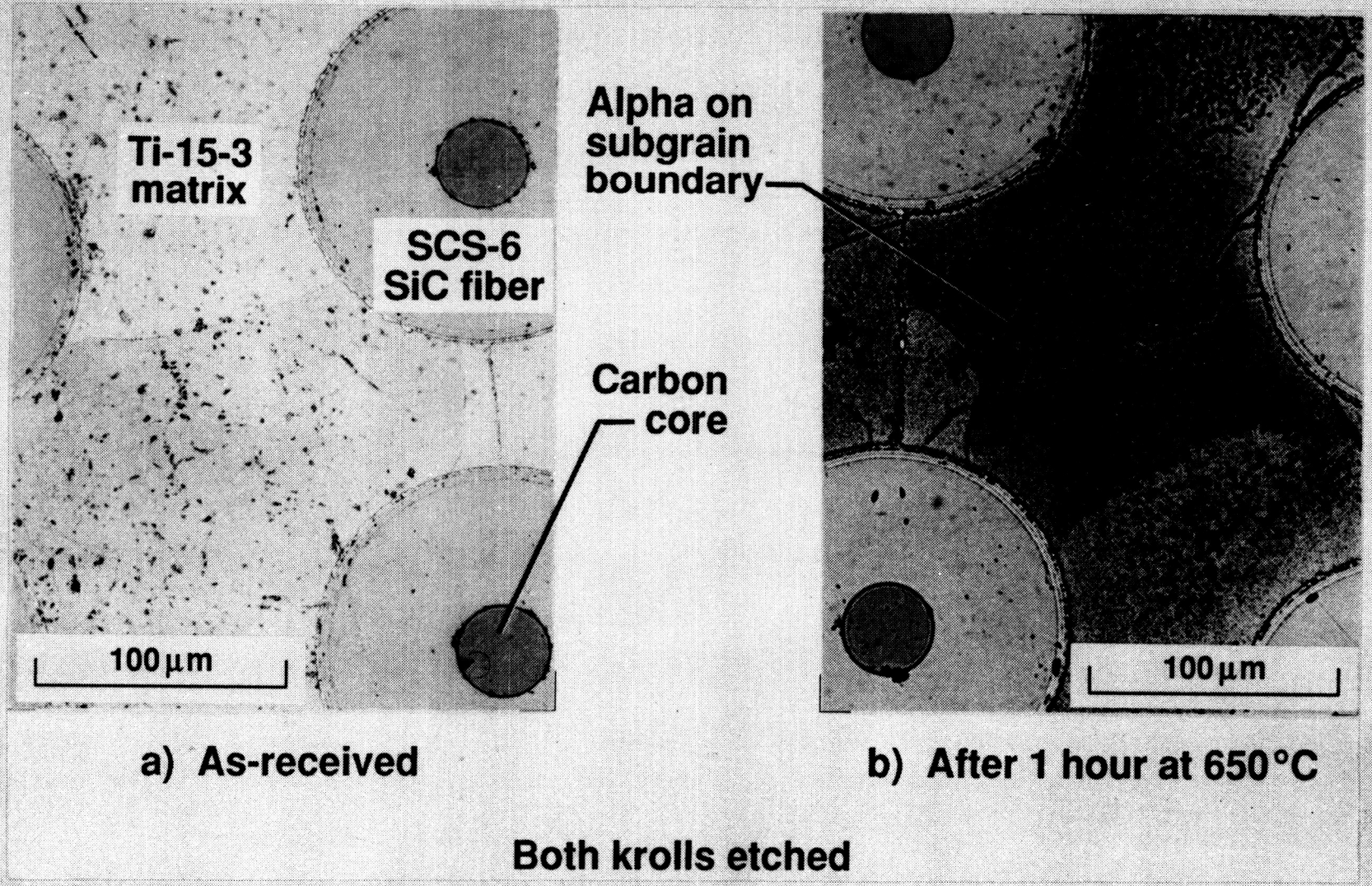

Figure 3. The microstructure of the SCS-6/Ti-15-3 composite. Both were etched with Krolls.

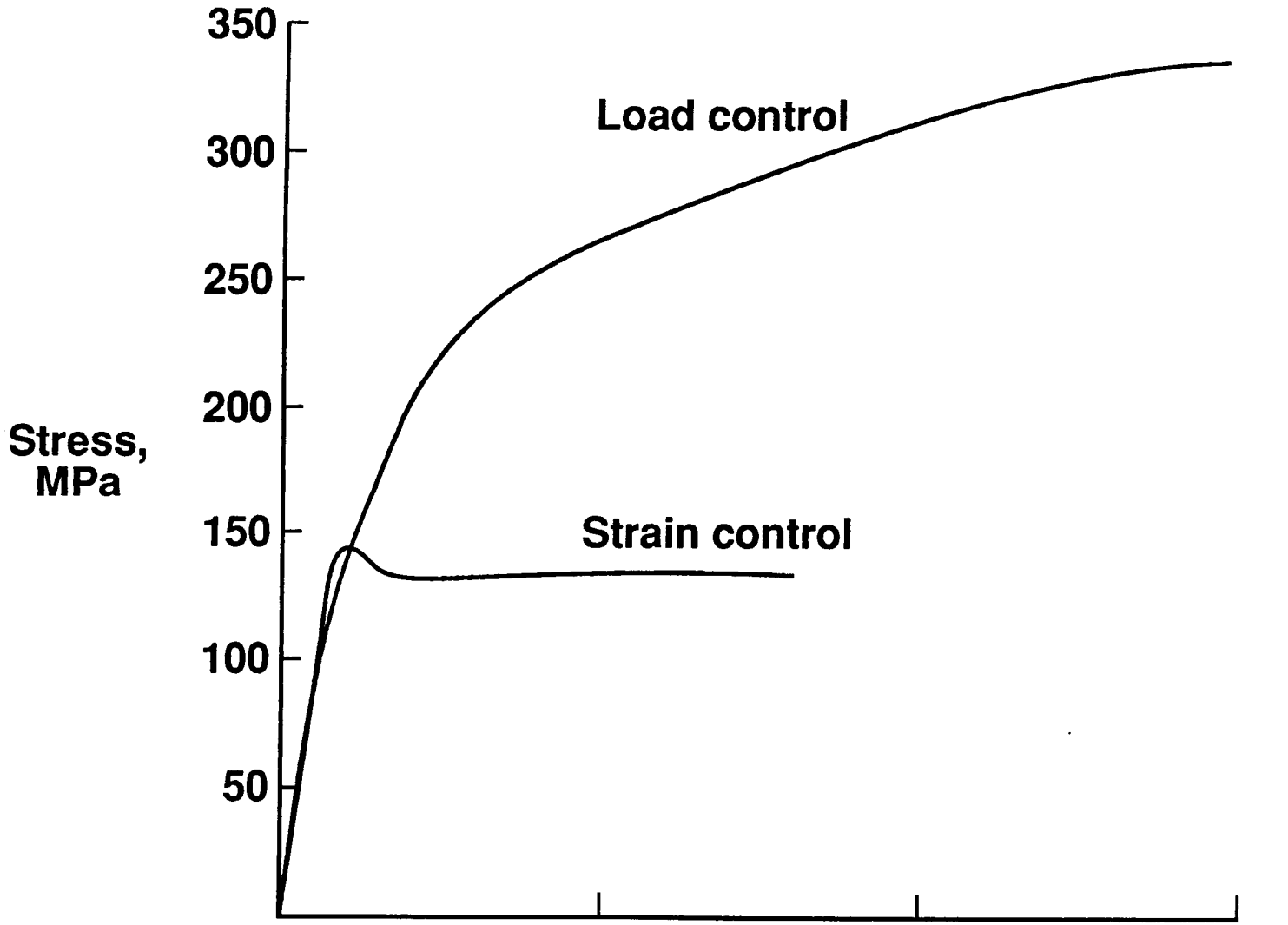

Figure 4. The stress-strain response of the matrix in strain and load control at 650°C.

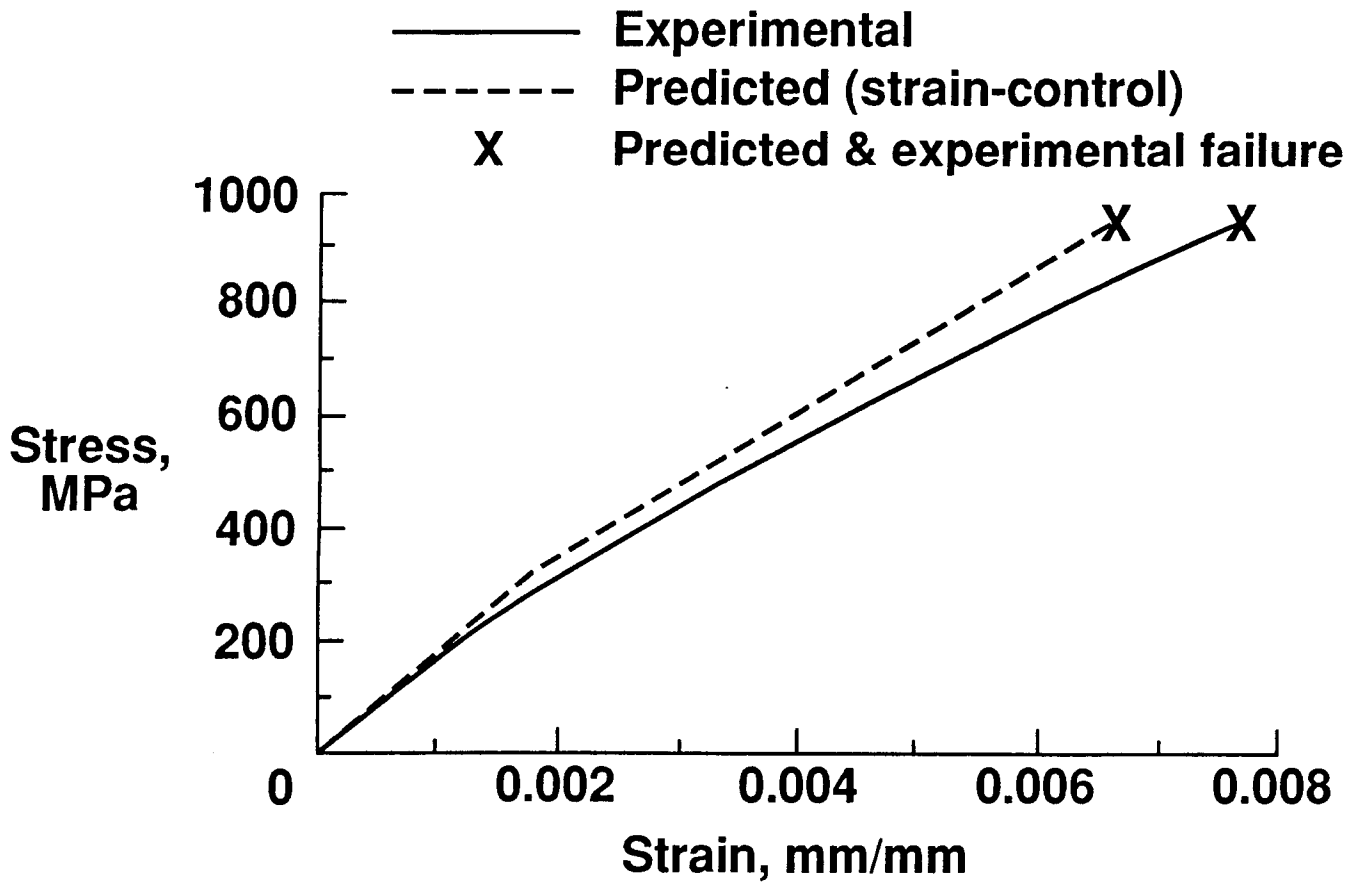

Figure 5. Unidirectional stress-strain response at elevated temperature.

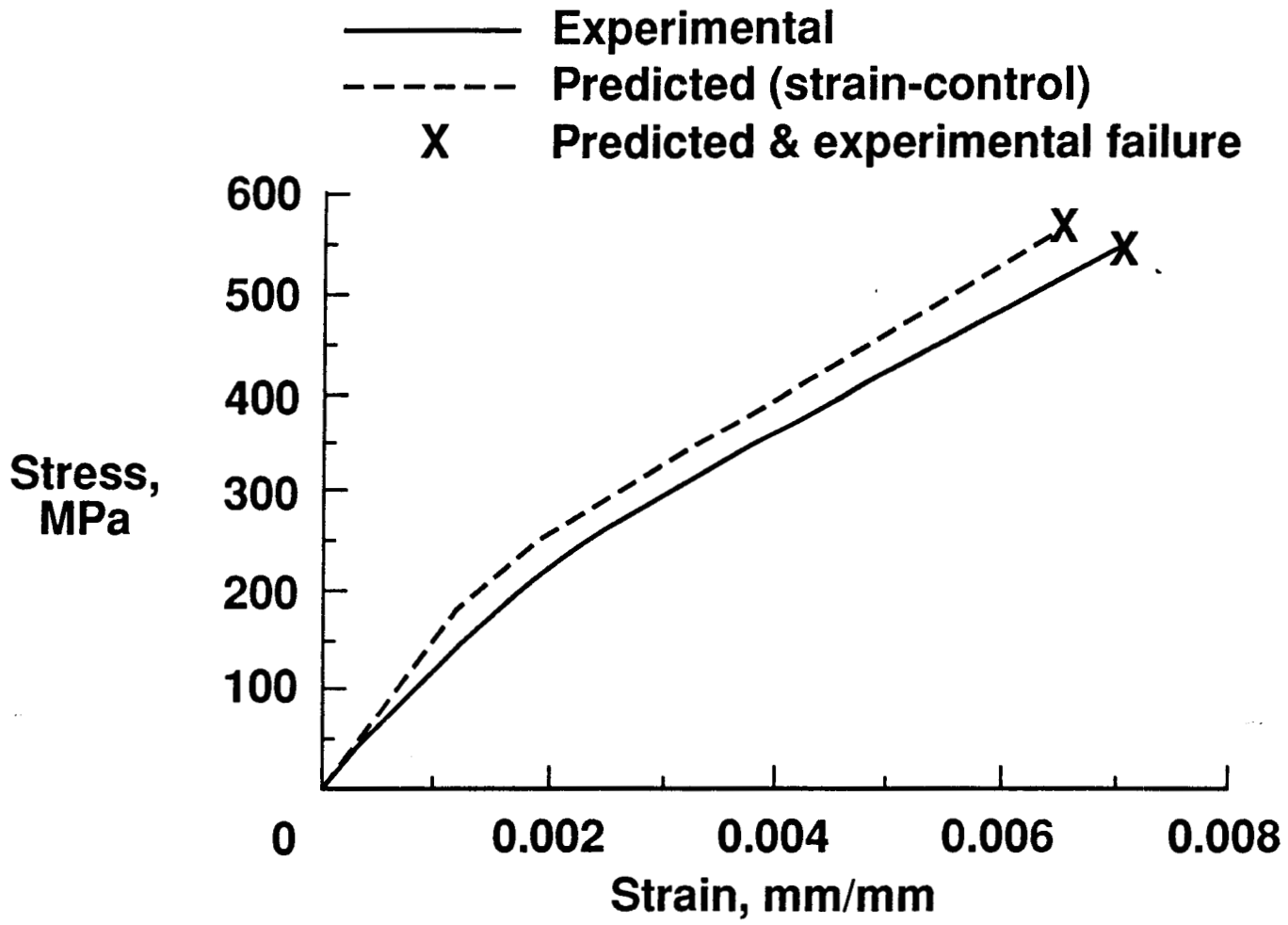

Figure 6. The $[0/90]_{2s}$ stress-strain response at elevated temperature.

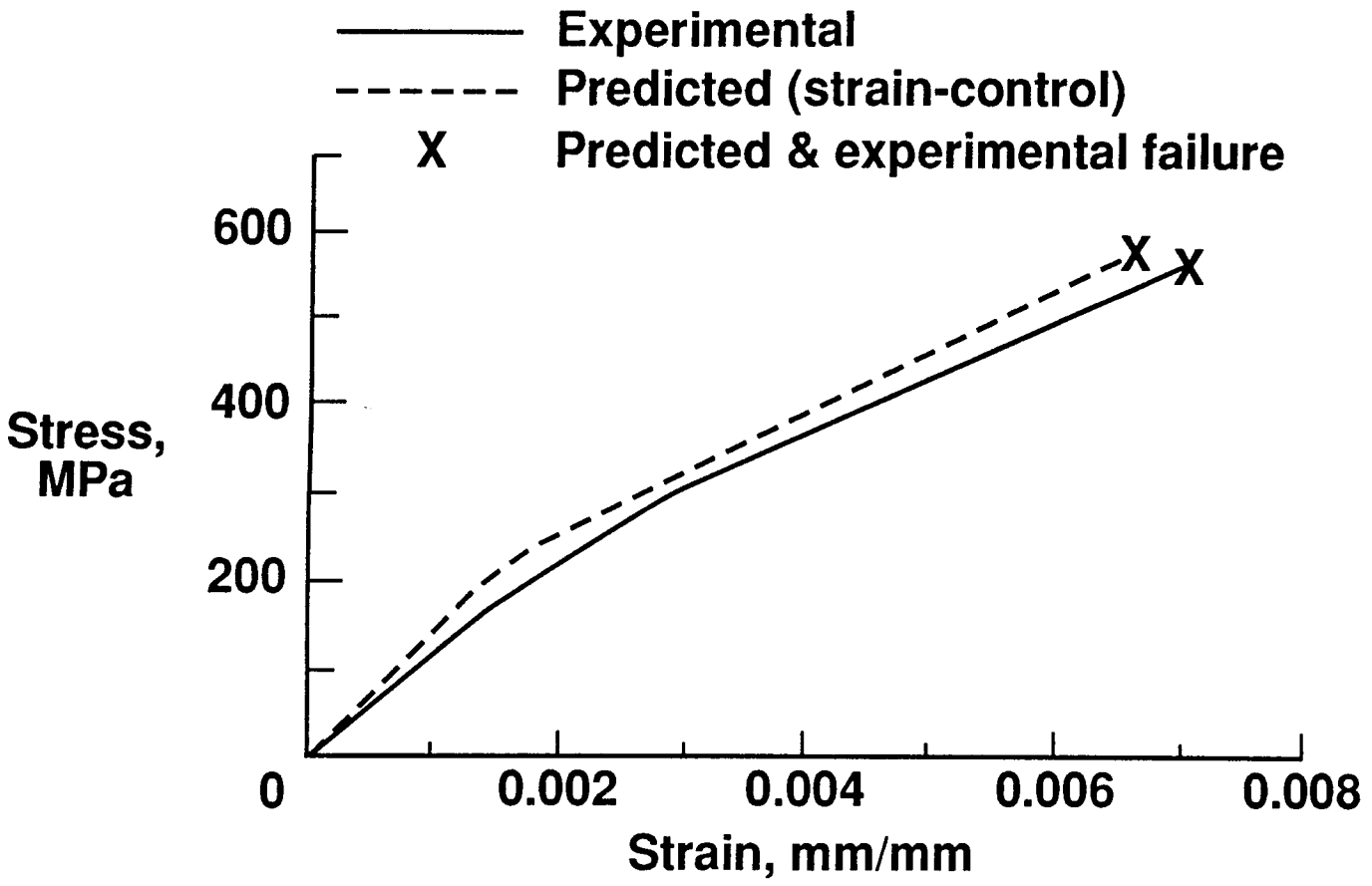

Figure 7. The $[0_2/\pm 45]_s$ stress-strain response at elevated temperature.

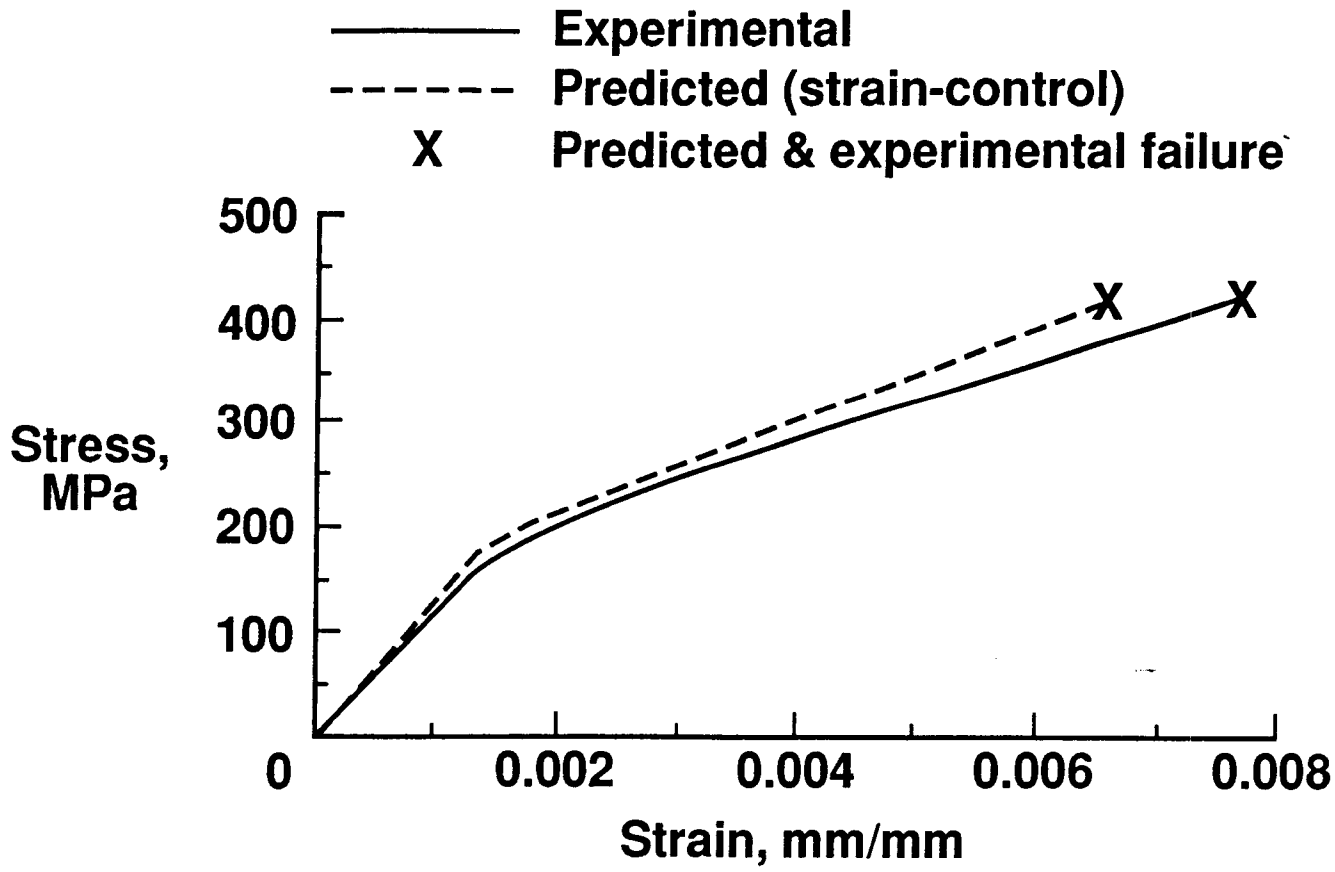

Figure 8. The $[0/\pm45/90]_s$ stress-strain response at elevated temperature.

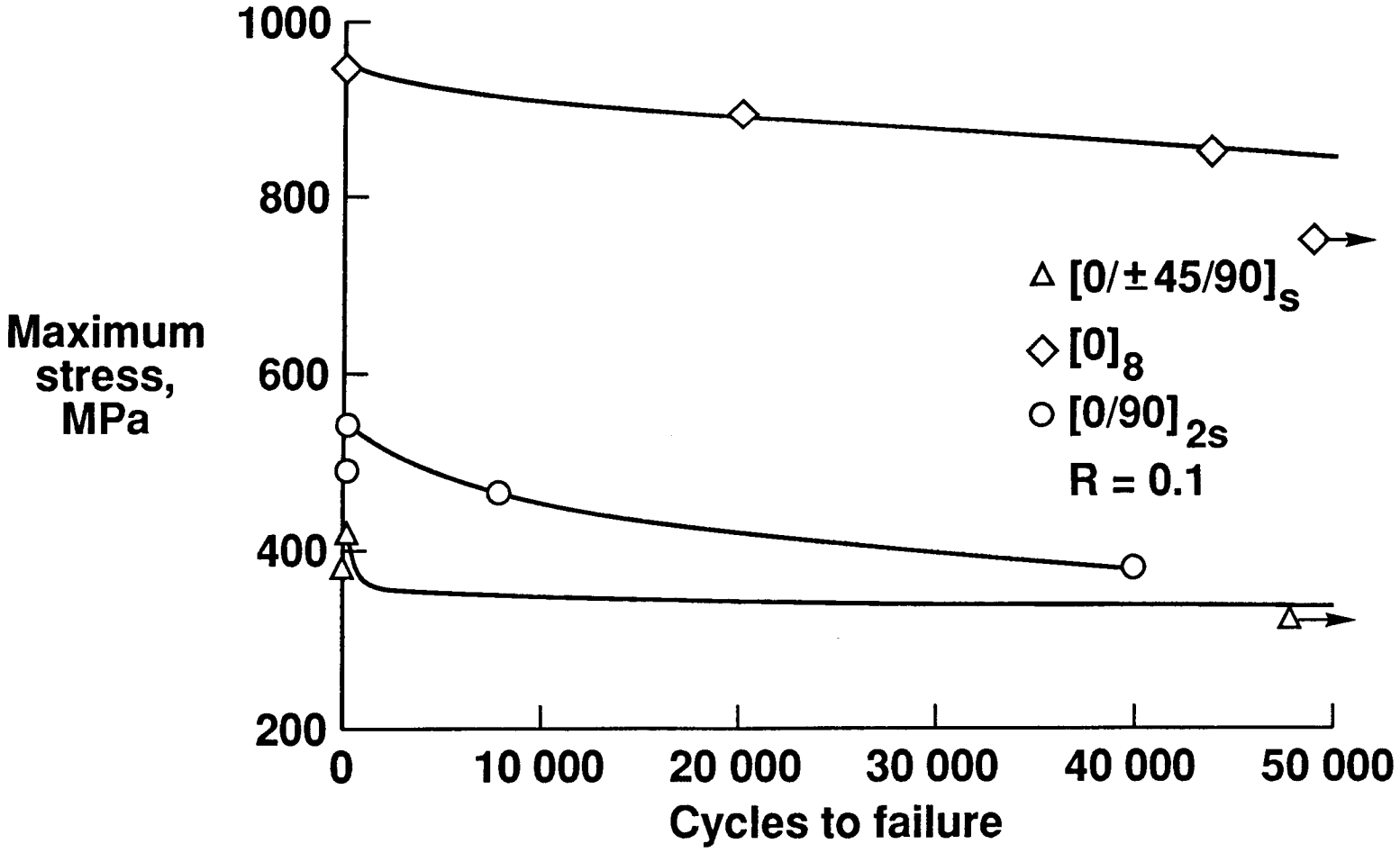

Figure 9. Cycles to failure for the SCS-6/Ti-15-3 composite at 650° C.

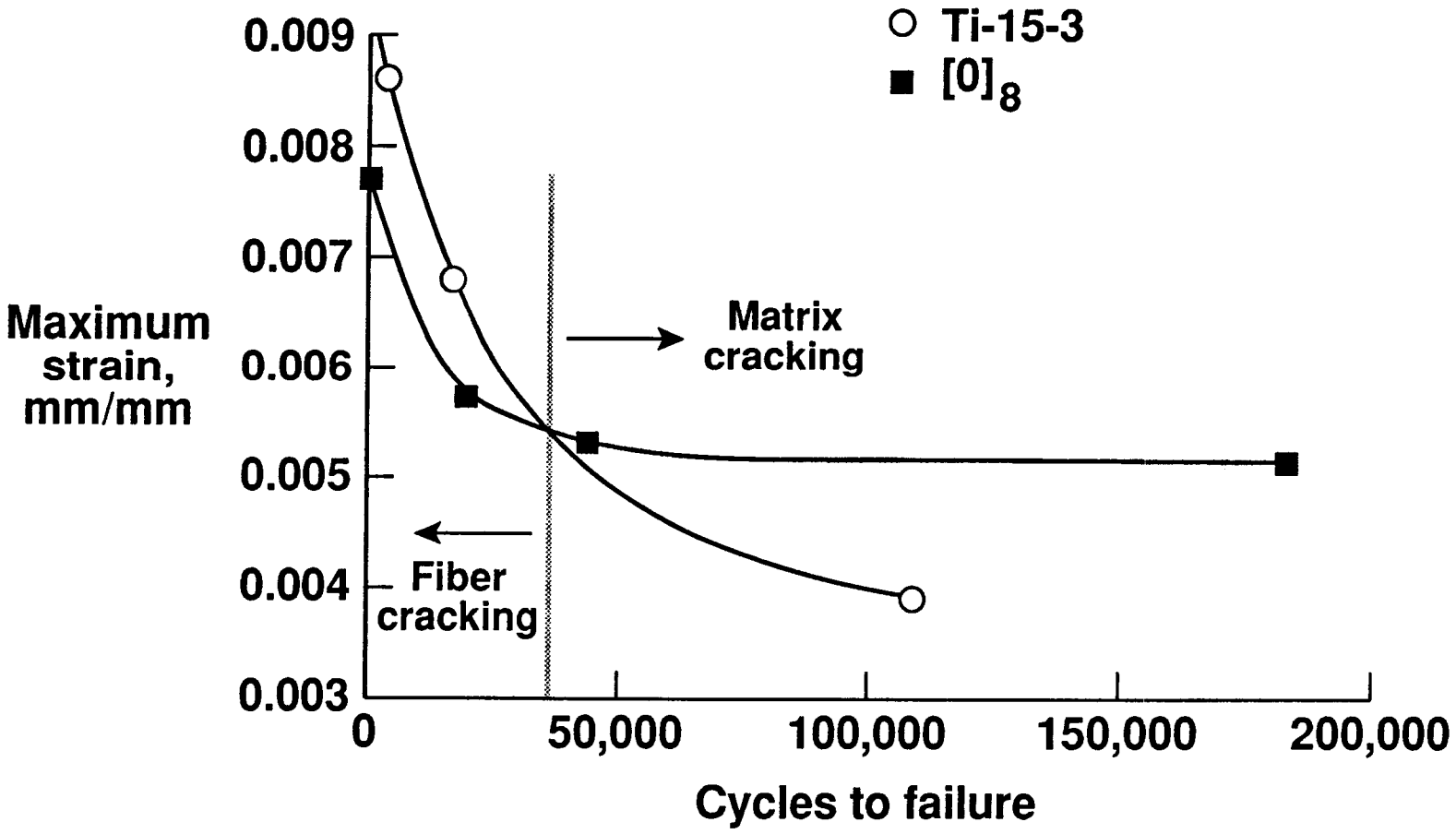

Figure 10. The life of the unidirectional composite and the matrix as a function of maximum strain at 650°C.

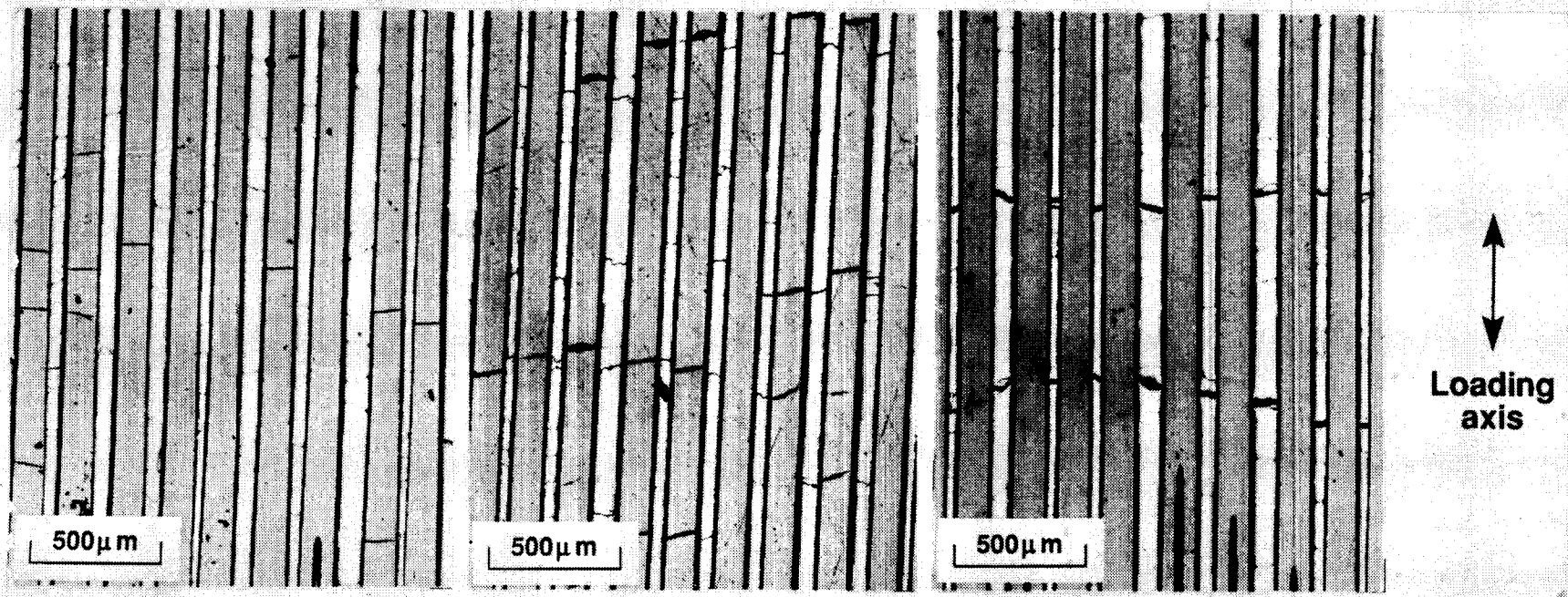

Figure 11. Sections parallel to the loading axis in unidirectional coupons behind the failed surface.

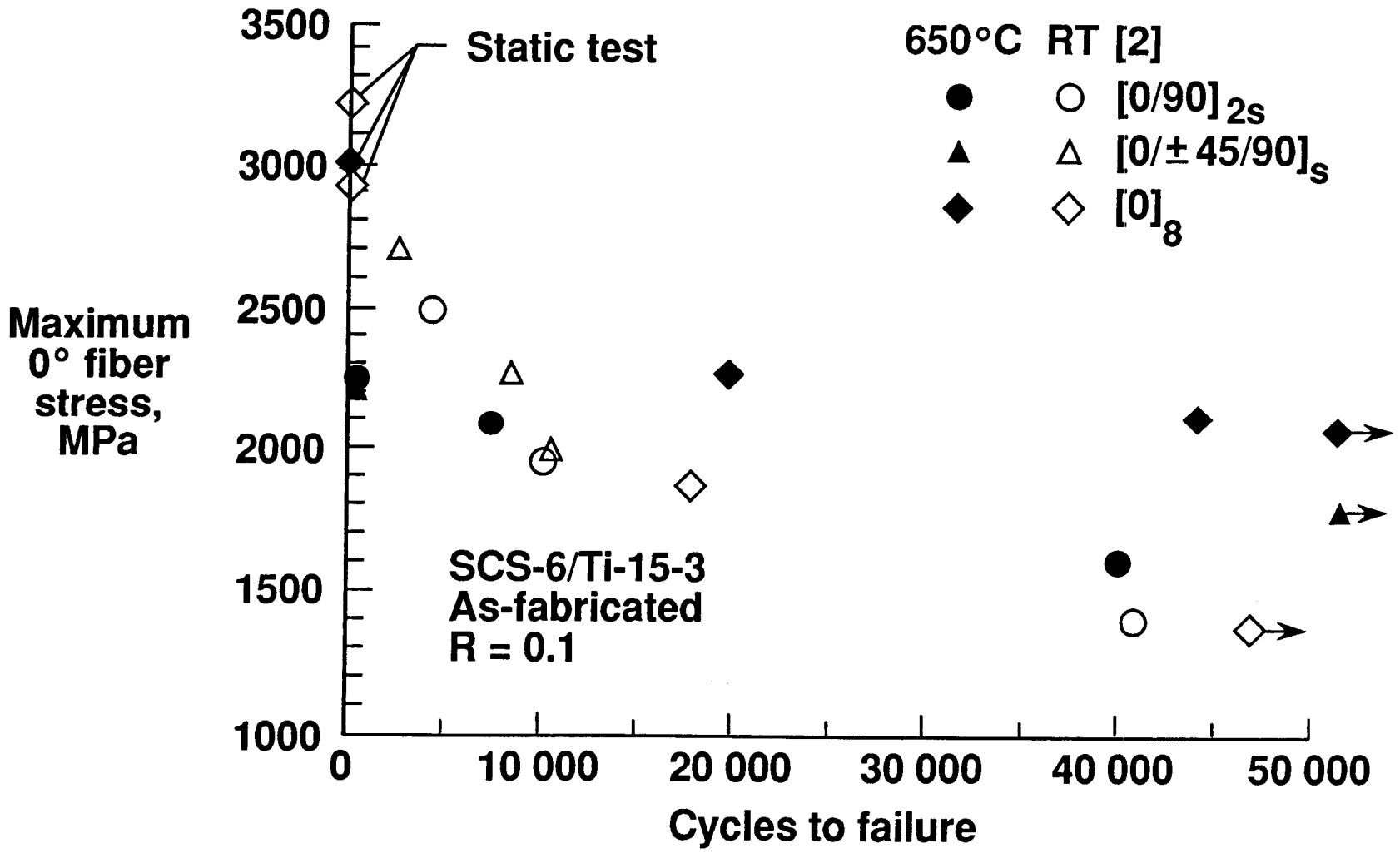

Figure 12. The stress in the 0° fiber as a function of cycles to failure for the various layups.

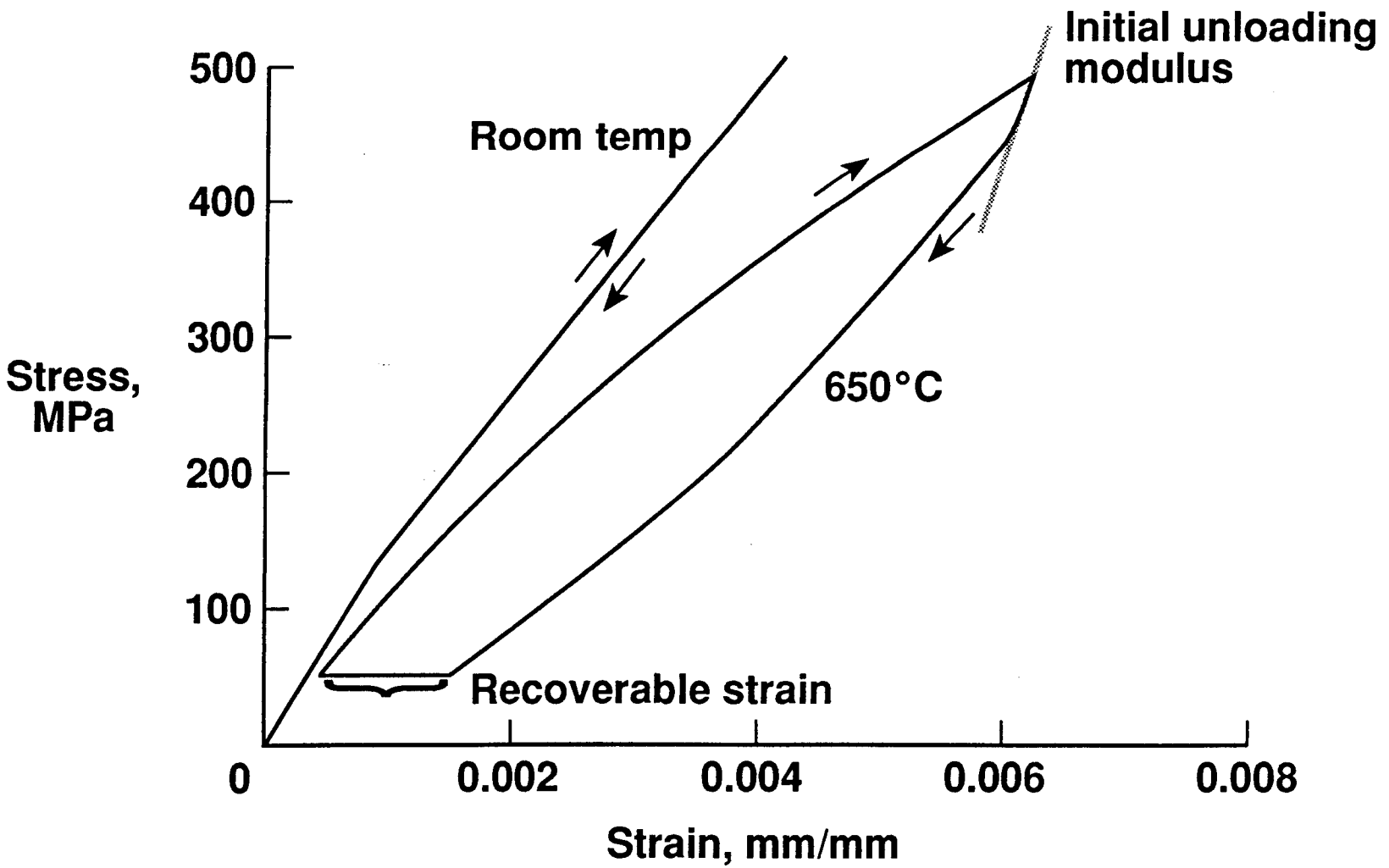

Figure 13. The cyclic response of the $[0/90]_{2s}$ layup at room temperature and 650°C.

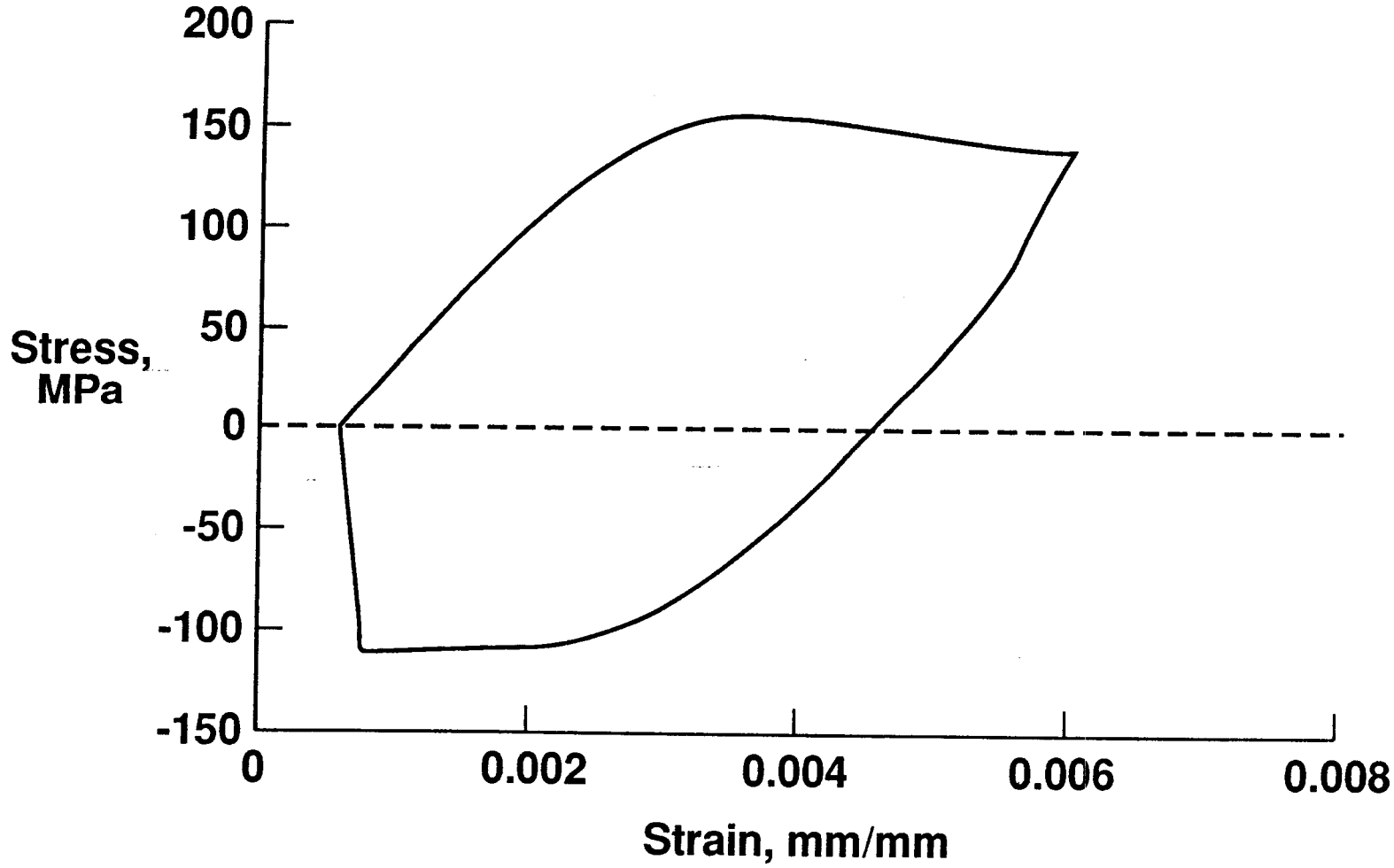

Figure 14. A strain-control cyclic test of the matrix at 650°C.

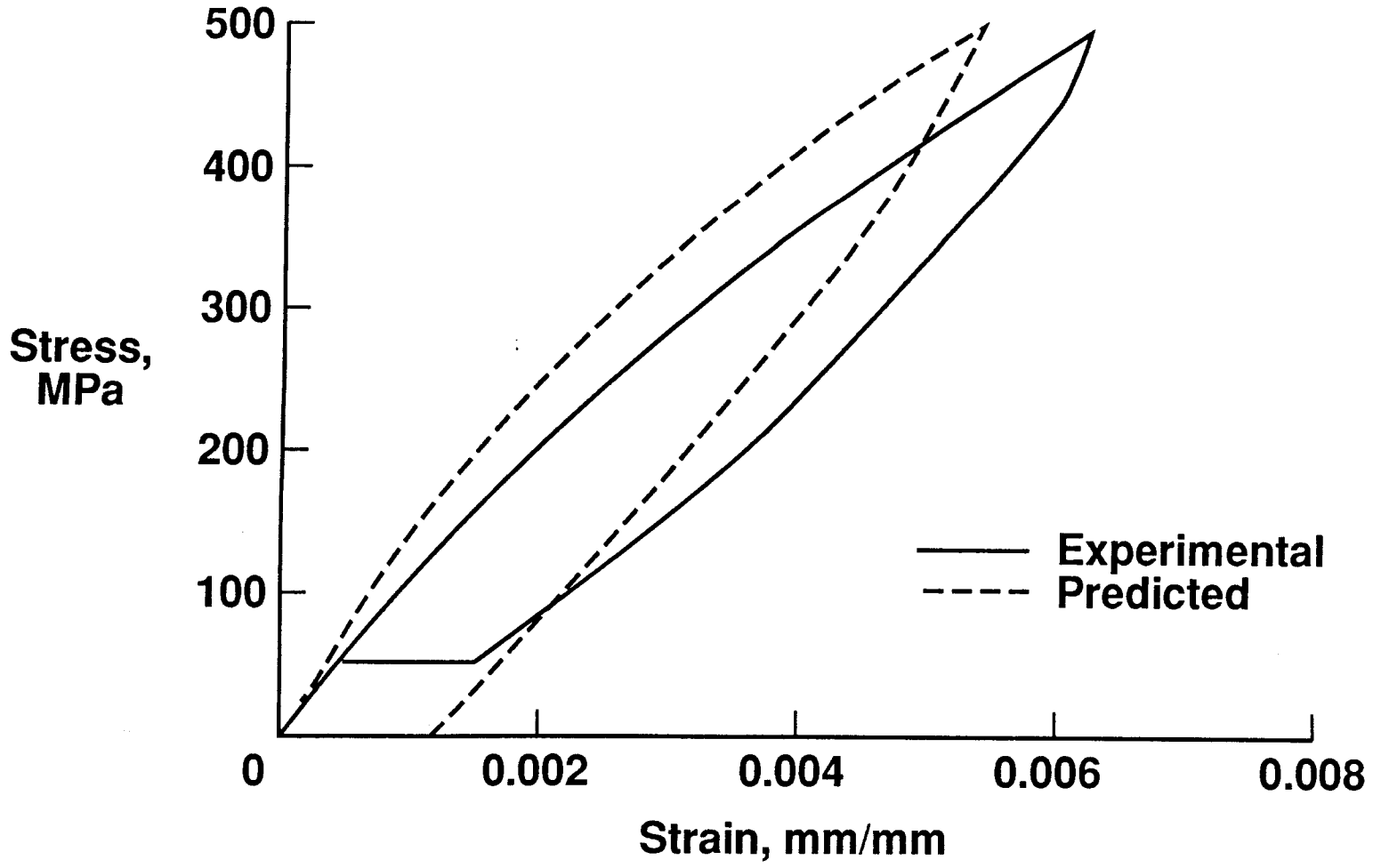

Figure 15. Predicted and experimental cyclic stress-strain response of the $[0/90]_{2s}$ layup at 650°C.

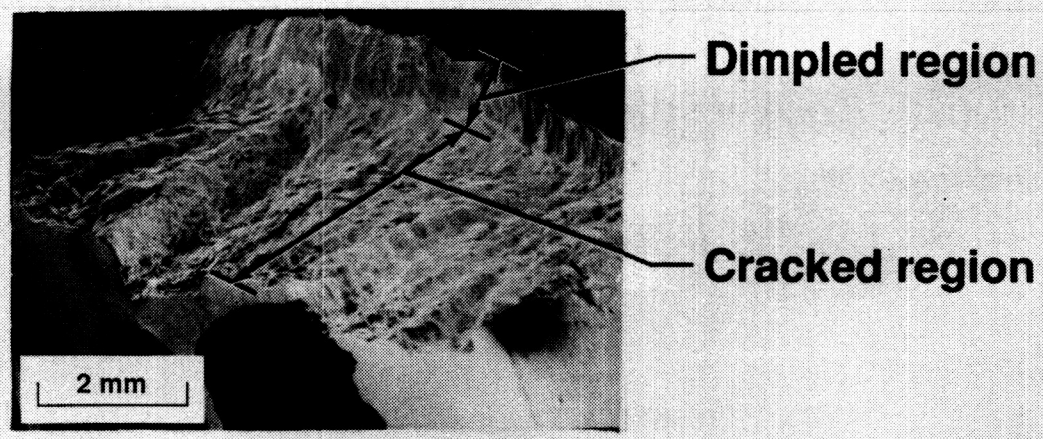

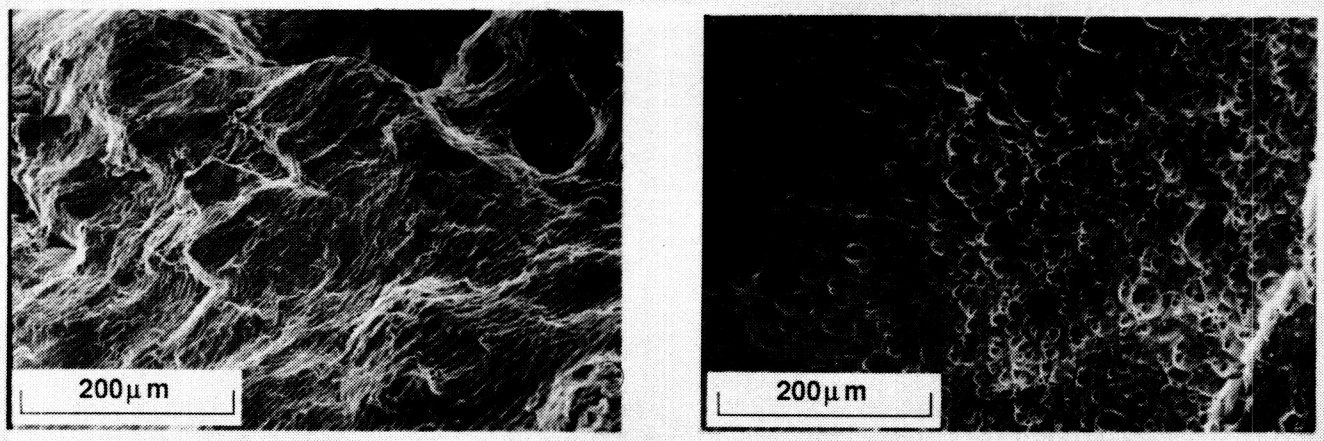

Figure 16. Fractograph from strain-controlled fatigue test of the matrix at 650°C. Cycled 109,000 times to failure with a maximum strain of 0.0047 mm/mm.

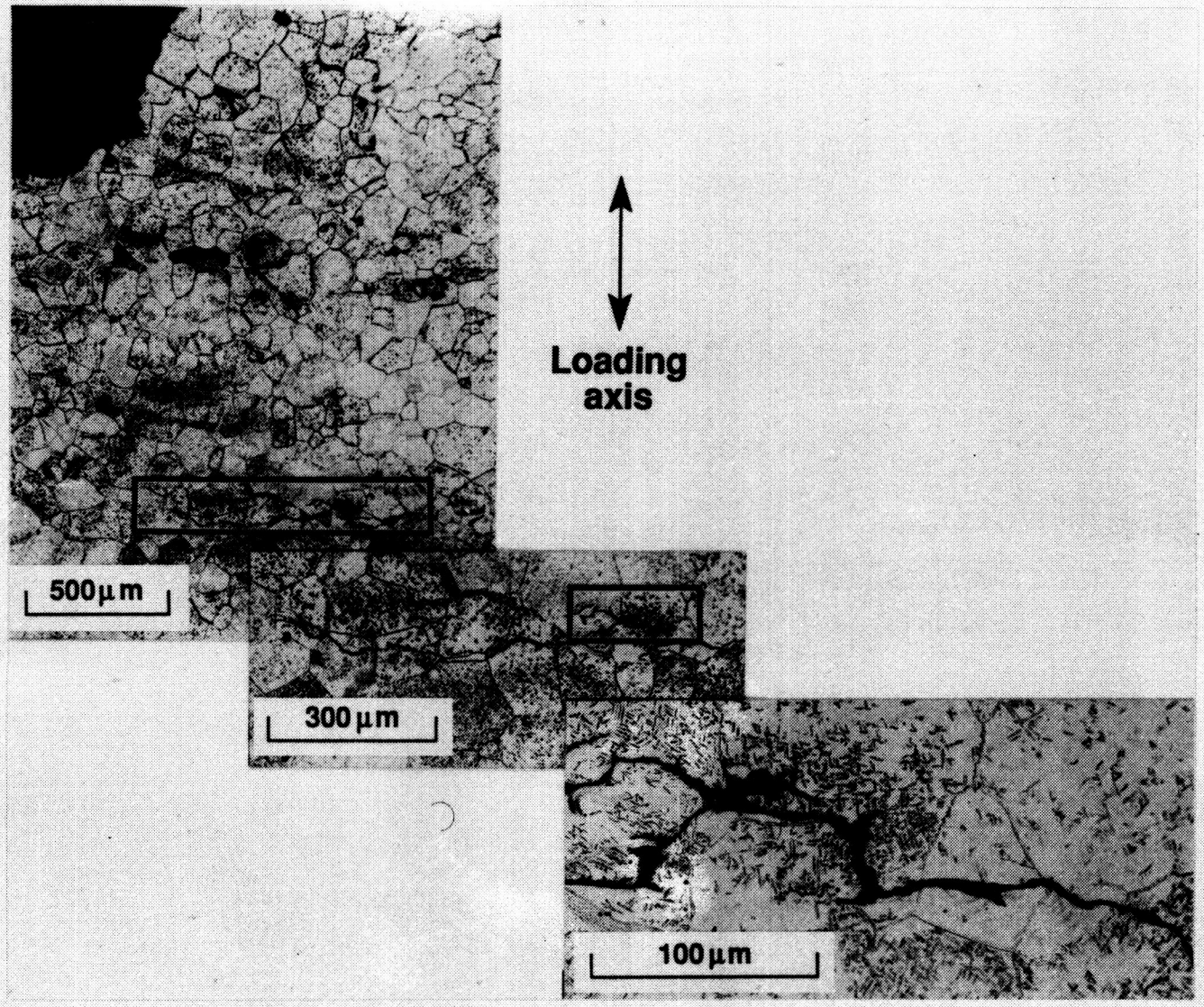

Figure 17. Transgranular cracking of the matrix at 650°C under strain-controlled cyclic loading. The grains are visible due to the Krolls etch. Sample was cycled 13,300 times to failure with a maximum strain of 0.0077 mm/mm.

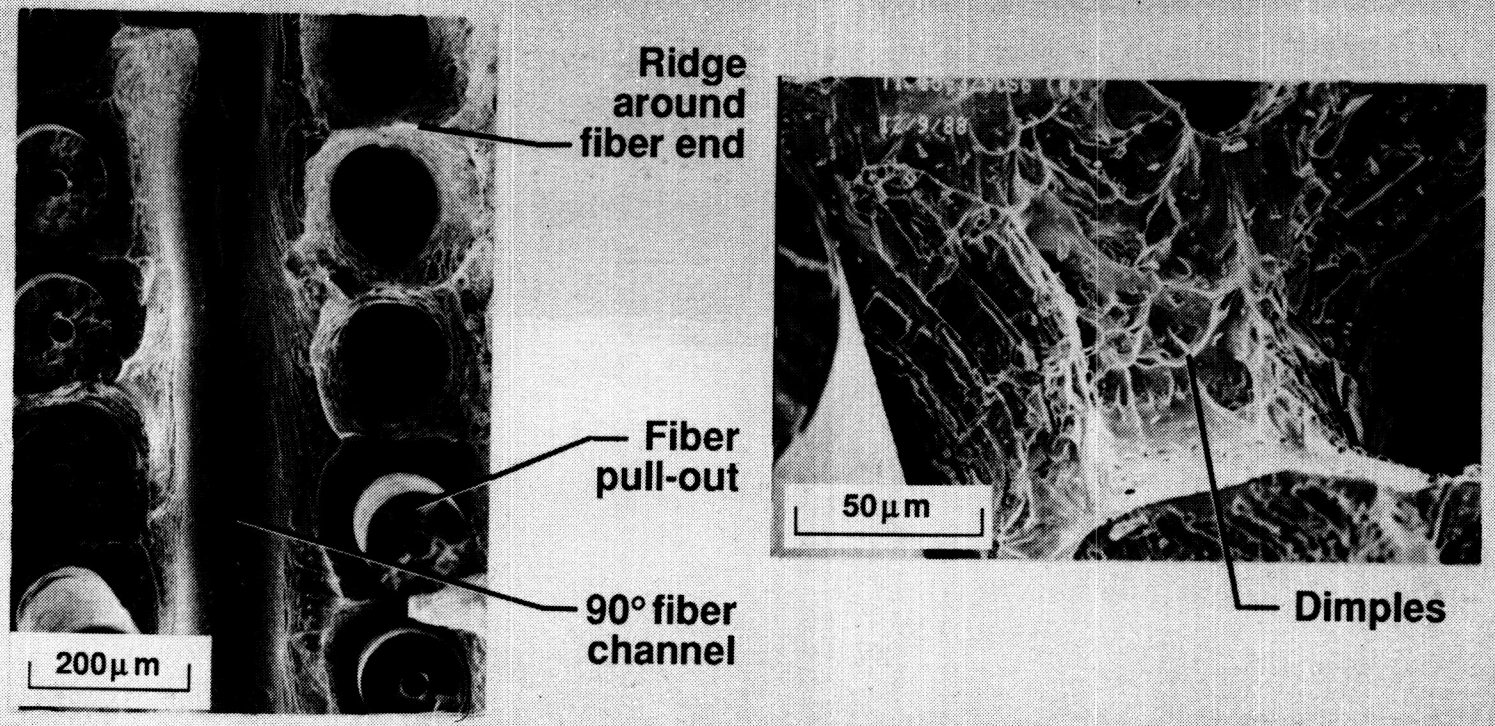

Figure 18. The monotonic tensile failure of the $[0/90]_{2s}$ composite at 650°C.

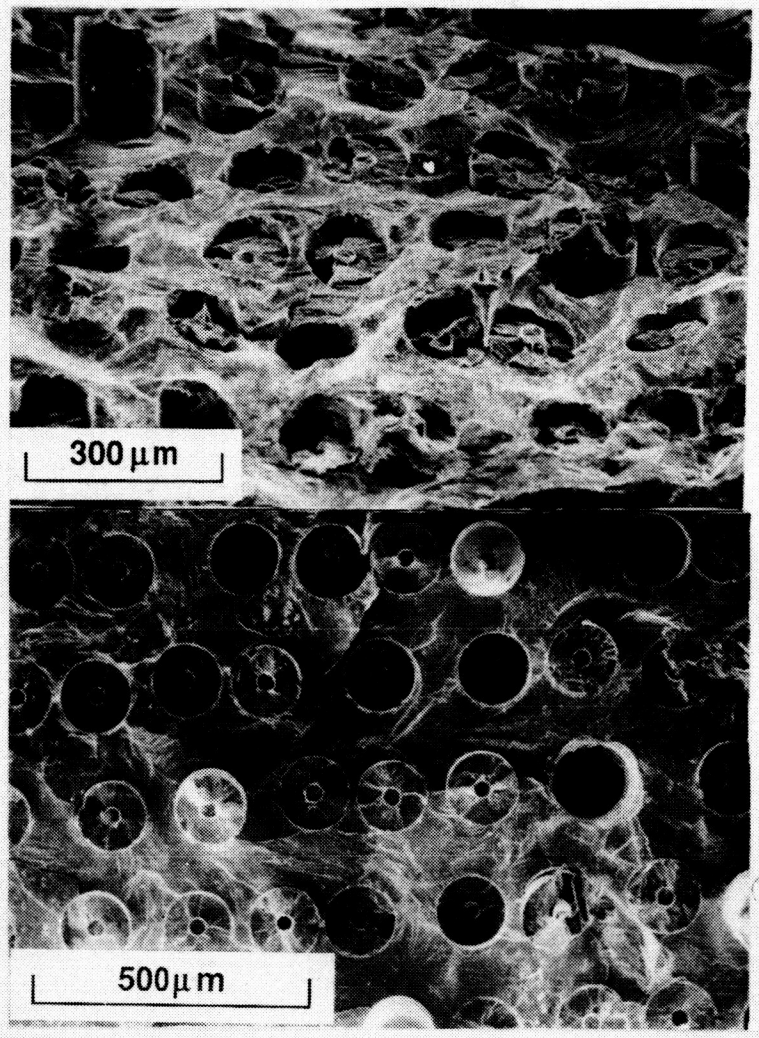

Figure 19. Fractograph of unidirectional composite cycled 183,000 times at a maximum stress of 758 MPa. The fractograph shows the flat matrix crack and the broken fibers close to the same plane.

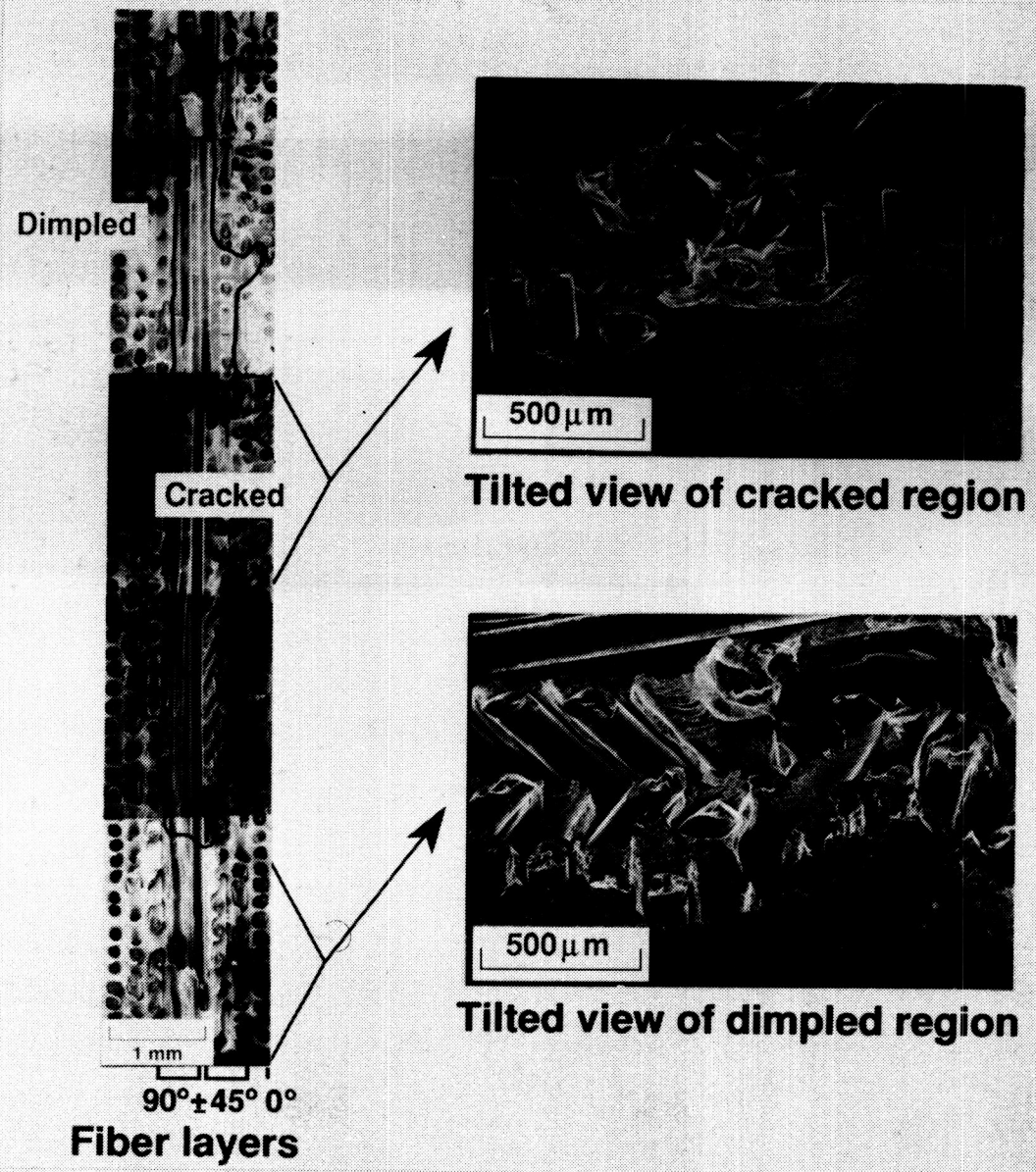

Figure 20. Extent of fatigue cracking in a $[0/\pm45/90]_s$ composite cycled 64,000 times at a maximum stress of 337 MPa.

NASA National Aeronautics and Space Administration

Report Documentation Page

1. Report No.	2. Government Accession No.	3. Recipient's Catalog No.
NASA TM-102699		

4. Title and Subtitle	5. Report Date
Characterization of Unnotched SCS-6/Ti-15-3 Metal Matrix Composites at 650°C	September 1990
	6. Performing Organization Code

7. Author(s)	8. Performing Organization Report No.
W. D. Pollock[1] and W. S. Johnson[2]	
	10. Work Unit No. 505-63-01-05

9. Performing Organization Name and Address	11. Contract or Grant No.
NASA Langley Research Center Hampton, VA 23665-5225	
	13. Type of Report and Period Covered: Technical Memorandum

12. Sponsoring Agency Name and Address	14. Sponsoring Agency Code
National Aeronautics and Space Administration Washington, DC 20546-0001	

15. Supplementary Notes

[1]Materials Engineer, Analytical Services and Materials, Inc, Hampton, VA

[2]Senior Research Engineer, NASA Langley Research Center, Hampton, VA

This paper was presented at the ASTM 10th Composite Materials Testing and Design Symposium, San Francisco, CA, April 23-25, 1990. Will be published in an ASTM STP of the same name.

16. Abstract

Ti-15-3 reinforced with SCS-6 silicon carbide fibers, in five different layups, was tested at 650°C to determine monotonic and fatigue strengths, basic mechanical properties, and damage initiation and progression. The elevated temperature results were compared to those obtained at room temperature. Analytical predictions were made of the monotonic stress-strain response as well as cyclic stress-strain hysteresis. The fiber reinforcement was found to significantly increase the static and fatigue strengths of the laminates over that of the matrix material at elevated temperature while the increase was insignificant at room temperature. Initial damage, in either the fibers or the matrix, was partitioned as a function of the life and applied strain range in the constituents. High strains and short lives resulted in multiple fiber failure with no signs of matrix fatigue cracking. Low strains and long lives resulted in extensive matrix cracking and no fiber breaks away from the fracture surface. At 650°C the matrix was too weak to cause fiber-matrix interface failure prior to matrix yielding. Laminate fatigue lives were hypothesized to be a function of the 0° fiber stress. More scatter was found in the 0° fiber stress vs. high temperature fatigue life data than for the room temperature data. An initial unloading modulus that was greater than the initial loading modulus was observed in the elevated temperature fatigue tests.

17. Key Words (Suggested by Author(s))	18. Distribution Statement
Titanium, Fatigue, Moduli, Creep, Elevated temperature, Silicon-carbide fibers	Unclassified - Unlimited Subject Category - 24

19. Security Classif. (of this report)	20. Security Classif. (of this page)	21. No. of pages	22. Price
Unclassified	Unclassified	36	A03

NASA FORM 1626 OCT 86